

# A simple mathematical model of cyclic hypoxia and its impact on hypofractionated radiotherapy

Edward Taylor

Princess Margaret Cancer Centre, University Health Network, Toronto, Canada  
Department of Radiation Oncology, University of Toronto, Toronto, Canada

April 18, 2022

edward.taylor@rmpuhn.ca

## Abstract

**Purpose:** There is now substantial evidence that the population of cells that experience fluctuating oxygen levels (“acute”, or, “cyclic” hypoxia) are more radioresistant than chronically hypoxic ones and hence, this population likely determines radiotherapy (RT) response, in particular for hypofractionated RT, where reoxygenation may not be as prominent. A considerable effort has been devoted to examining the impact of hypoxia on hypofractionated RT; however, much less attention has been paid to cyclic hypoxia specifically and the role its kinetics may play in determining the efficacy of these treatments. Here, a simple mathematical model of cyclic hypoxia and fractionation effects was worked out to quantify this.

**Methods:** Cancer clonogen survival fraction was estimated using the linear quadratic model, modified to account for oxygen enhancement effects. An analytic approximation for oxygen transport away from a random network of capillaries with fluctuating oxygen levels was used to model inter-fraction tissue oxygen kinetics. The resulting survival fraction formula was used to derive an expression for the iso-survival biologically effective dose,  $\text{BED}_{\text{iso-SF}}$ . These were computed for some common extra-cranial hypofractionated radiotherapy regimens.

**Results:** Using relevant literature parameter values, inter-fraction fluctuations in oxygenation were found to result in an added 1-2 logs of clonogen survival fraction in going from five fractions to one for the same nominal biologically effective dose (i.e., excluding the effects of oxygen levels on radiosensitivity).  $\text{BED}_{\text{iso-SF}}$ ’s for most ultra-hypofractionated (five or fewer fractions) regimens in a given tumour site are similar in magnitude, suggesting iso-efficacy for common fractionation schedules.

**Conclusions:** Although significant, the loss of cell-killing with increasing hypofractionation is not nearly as large as previous estimates based on the assumption of complete reoxygenation between fractions. Most ultra-hypofractionated regimens currently in place offer sufficiently high doses to counter this loss of cell killing, although care should be taken in implementing single-fraction regimens.

It is well-known that cells at low oxygen tensions (“hypoxia”) are more radioresistant than those at higher oxygen levels, with as much as three times more dose required to achieve the same level of cell killing<sup>1,2</sup> and hence, the presence of hypoxia in a tumour likely plays a key role in determining the response to radiation therapy (RT)<sup>3</sup>. Several experiments have demonstrated, either indirectly<sup>4,5</sup> or directly<sup>6</sup>, that this reduction in sensitivity is transient, however: cells that are chronically ( $\gtrsim$  days) hypoxic exhibit a more modest dose-enhancing factor of  $\sim 1.4$  as compared to the factor of 2.5-3 experienced by cells that are transiently hypoxic, likely the result of impaired ability to repair radiation-induced DNA damage<sup>6</sup>. There is substantial pre-clinical evidence showing that most tumours harbor a radiobiologically significant population of such transiently hypoxic cells, an effect often referred to as acute or cyclic hypoxia<sup>4,7,8,9,10,11</sup>.

Assuming that this population exists in clinical populations (and there is only indirect evidence of this; see the recent review by Bader *et al.*<sup>11</sup>), we thus hypothesize that it is the cyclically hypoxic component and its kinetics through treatment that determine RT response. To see this, let us stratify the clonogens in a tumour into three compartments: an oxic, and cyclically and chronically hypoxic compartments, each with their own oxygen enhancement ratio (OER) describing the factor by which dose needs to be increased to achieve the same cell killing as under oxic conditions:  $OER_{\text{oxic}} = 1$ ,  $OER_{\text{chronic}} = 1.37$ , and  $OER_{\text{cyclic}} = 2.5$ <sup>6</sup>. Further suppose that cells in these compartments are subject to a dose  $d$  per fraction over  $N$  fractions and that the surviving fraction (SF) of clonogens can be described by the linear-quadratic (LQ) model, modified to account for oxygen enhancement effects<sup>2,12,13</sup>. Assuming that the oxygen level experienced by each clonogen remains constant in time, the SF in each compartment is given by:

$$SF_i \equiv e^{-\alpha \cdot \text{BED}_i(N)}, \quad i = \text{oxic, cyclic, chronic} \quad (1)$$

Here,  $\alpha$  is the intrinsic radiosensitivity parameter and

$$\text{BED}_i(N) \equiv \frac{Nd}{\text{OER}_i} \left( 1 + \frac{d}{(\alpha/\beta)\text{OER}_i} \right). \quad (2)$$

is the compartment-specific biologically effective dose (BED)<sup>12</sup>, with  $\alpha/\beta$  quantifying the intrinsic sensitivity to fractionation effects. Using  $\alpha = 0.4 \text{ Gy}^{-1}$ ,  $\alpha/\beta = 10 \text{ Gy}$ ,  $d = 12 \text{ Gy}$ , and  $N = 4$  (a standard fractionation regimen for early-stage non-small-cell lung cancer),  $SF_{\text{oxic}} \sim 10^{-19}$ ,  $SF_{\text{chronic}} \sim 10^{-12}$ , and  $SF_{\text{cyclic}} \sim 10^{-5}$ . For comparison, the tumour control

probability (TCP) can be related to SF by  $TCP \sim \exp(N_c \cdot SF)$ <sup>14</sup>, where  $N_c$  is the number of clonogens. To achieve 50% tumour control probability for a  $10 \text{ cm}^3$  tumour with a clonogen density between  $10^6$  and  $10^8 \text{ cm}^{-3}$  (see Tomé *et al.*<sup>14</sup> and Søvik *et al.*<sup>15</sup>) would require a survival fraction between  $10^{-7}$  and  $10^{-9}$ . Thus, ignoring kinetic changes to oxygen levels through our simulated 48 Gy in four fraction RT regimen, the surviving cells will belong to the cyclically hypoxic compartment and it is this population that prevents tumour control.

The cyclically hypoxic compartment is of course not static, fluctuating as often as several times per hour<sup>11</sup>. Hence, we anticipate that the inter-fraction kinetics of cyclic hypoxia is a major factor determining the fraction of cells surviving hypofractionated RT. Historically, the large OER of the hypoxic compartment was assumed to be mitigated during conventionally fractionated radiotherapy ( $N \gtrsim 20$ ) by “reoxygenation”, the process by which cells that are hypoxic early in RT gradually become oxic at subsequent fractions, rendering them more radiosensitive<sup>16</sup>. Technological advances over the past two decades have led to the adoption of hypofractionated RT regimens such as stereotactic body radiotherapy (SBRT), lasting five or fewer fractions. While some reoxygenation (here defined as a reduction in the volumetric average of the oxygen tension in a tumour) may occur during these abbreviated regimens<sup>17</sup>, it is not clear that it is sufficient to mitigate the impact of hypoxia and cyclic hypoxia may play a greater role.

In this paper, we develop a probabilistic model of cyclic hypoxia to quantify its impact on hypofractionated RT. A number of authors have examined the effect of hypoxia on hypofractionated RT<sup>18,19,20,21,22,23,24,25,26,27</sup>. Comparatively little attention seems to have been paid to modelling the specific impact of cyclic hypoxia, however. Popple and colleagues<sup>28</sup>, while not explicitly studying hypofractionated RT, quantified the influence of cyclic and chronic hypoxia by modelling the former as a completely stochastic population; i.e., by assuming that cells randomly shuttle between oxic and cyclic hypoxia compartments at each fraction. Ruggieri *et al.* studied the affect of cyclic hypoxia on hypofractionated RT by assuming that cells in the cyclic hypoxia compartment oscillated between oxic and hypoxic states periodically in time with randomly assigned phases<sup>19,29</sup>. Toma-Daşu and colleagues calculated cancer clonogen survival by simulating oxygen diffusion and metabolism from simulated capillary networks; acute hypoxia was simulated by randomly closing a fraction of simulated capillaries between each fraction<sup>22,30</sup>.

Although differing in some details, the approach taken by us here is conceptually similar to that of these last two references<sup>22,30</sup>. A key feature of these works is the spatial aspect of their modelling, via calculations of oxygen metabolism and diffusion for simulated vascular architectures. This is important because, in contrast to purely stochastic approaches, cells that are in well-perfused regions are unlikely to oscillate between extremes of hypoxia and oxia between fractions while cells that are far from blood vessels are likewise unlikely to become oxic. The probability that a cell is oxic or hypoxic at a given fraction is thus not independent of the oxygenation status at previous fractions, since both are functions of the local vascular architecture. Mathematically, this lack of complete stochasticity lessens the impact of decreasing fractionation: for completely stochastic oxygenation dynamics, the probability that a given cell is hypoxic—and hence, maximally radioresistant—over the entire treatment diminishes rapidly with increasing fraction number  $N$  as  $p^N$ , where  $p$  is the probability that the cell is hypoxic at a single fraction. (This applies not only to cyclic hypoxia but also assumptions of complete “stochastic” reoxygenation of a chronically hypoxic compartment between fractions<sup>20</sup>). In contrast, modelling the expected non-stochasticity of tissue oxygen tension, the probability that a cell is hypoxic for the duration of RT decays more slowly with  $N$ .

The non-stochastic nature of hypoxia dynamics may be of relevance for understanding the apparent success of *ultra*-hypofractionated regimes ( $N \leq 5$ ): if the spatial-temporal kinetics of hypoxia are completely stochastic, one would expect a substantial decrease in tumour control in going e.g., from five fractions to a single one, unless this reduction were accompanied by a substantial increase in dose. Although ultra-hypofractionation has largely been accompanied by increases in doses (as briefly reviewed in Section III.), these are not sufficient to overcome the loss of cell killing implied by completely stochastic oxygen kinetics. By using a simple approximation to the full oxygen metabolism-diffusion problem<sup>22,30</sup> in the present work, we derive analytic expressions for the clonogen survival fractions and iso-survival fraction doses under cyclically hypoxic conditions that we hope will facilitate analysis of fractionation schedules and give insight into the key parameters that control the magnitude of cyclic hypoxia’s impact.

We begin by introducing our model of cyclic hypoxia in Section I. Although it assumes stochastic temporal dynamics in capillary oxygen levels, by incorporating the spatial dependency of hypoxia with respect to the capillary architecture in an approximate way, this

model captures the non-stochasticity of tissue oxygen levels described above. In Section II., we combine this model with the LQ model to obtain an analytic expression for clonogen survival as a function of the chosen fractionation regimen and the amplitude of cyclic hypoxia. We close in Section III. by discussing the implications of our results for some modern hypofractionated SBRT regimens currently in use for lung, liver, pancreas, and prostate cancers, and propose a method to combat cyclic hypoxia.

## I. Cyclic hypoxia model

Acute or cyclic hypoxia arises from transient fluctuations in red blood cell flux<sup>7,8,9,31</sup>. The impact of a reduced blood cell flux through capillaries is to reduce the oxygen tension  $p_c$  inside the capillaries<sup>9</sup>, the value determined by the interplay between the number of red blood cells entering a region per unit time (flux) and the rate of oxygen metabolism in the tissue there. Fluctuations in  $p_c$  yield fluctuations in tissue oxygen levels, yielding cyclic hypoxia. Experiments have shown that cyclic hypoxia is spatially correlated over domains approximately 200-300  $\mu\text{m}$  in extent<sup>31</sup>, implicating an “upstream”<sup>9</sup> effect such as thermoregulation-induced vasomotion<sup>11</sup> that simultaneously impacts groups of microvessels.

A key quantity entering this work is the hypoxic fraction, denoted by  $\text{HF}_\Lambda$ , describing the fraction of tissue for which the local oxygen tension  $p(\mathbf{r})$  at a point  $\mathbf{r}$  is less than a radiobiologically relevant threshold oxygen tension  $\Lambda$ . Given the spatial extent of cyclic hypoxia correlations, for our purposes, it will be useful to define  $\text{HF}_\Lambda$  as the fraction of tissue in a pseudo-voxel several hundred  $\mu\text{m}$ ’s in size. Note that this differs from standard nomenclature, wherein hypoxic fraction refers to the fraction of tissue within an entire tumour for which  $p(\mathbf{r}) < \Lambda$ . Amongst other factors, the oxygen level  $p(\mathbf{r})$  in tissue is a function of that in capillaries,  $p_c$ . By defining this “microscopic” hypoxic fraction, we can associate a voxel-specific value  $p_c(t)$  of the time-varying capillary oxygen tension to all tissue in that pseudo-voxel and hence, express the hypoxic fraction there as a function of this  $p_c(t)$ :  $\text{HF}_\Lambda = \text{HF}_\Lambda(p_c)$ . Since the oxygen enhancement ratio rises rapidly below 5 mmHg<sup>12</sup>, an appropriate choice of cutoff  $\Lambda$  should be on the order of several mmHg’s.

Now, suppose that  $p_c$  cycles (possibly irregularly) between minimum and maximum values of capillary oxygen tension, denoted by  $p_{c,\min}$  and  $p_{c,\max}$ , respectively. The fraction

$\text{HF}_{\text{chronic}}$  of tissue that is *chronically* hypoxic refers to the fraction of tissue in a pseudo-voxel that is always hypoxic ( $p < \Lambda$ ):

$$\text{HF}_{\text{chronic}} \equiv \text{HF}_{\Lambda}(p_{c,\text{max}}). \quad (3)$$

Correspondingly, the *potential* cyclic hypoxic fraction

$$\text{HF}_{\text{pot.}} \equiv \text{HF}_{\Lambda}(p_{c,\text{min}}) - \text{HF}_{\Lambda}(p_{c,\text{max}}) \quad (4)$$

is defined as the fraction of non-chronically hypoxic tissue that, given enough time, is guaranteed to cycle between oxic ( $p > \Lambda$ ) and hypoxic ( $p < \Lambda$ ) states. This quantity in general differs from the *mean* cyclic hypoxic fraction  $\langle \text{HF}_{\text{cyclic}} \rangle$ , which is the expectation value of the fraction of non-chronically hypoxic tissue for which  $p(\mathbf{r}) < \Lambda$  *at any point in time*. We assume that the  $p_c$  values in each pseudo-voxel and at each time-point (fraction) fluctuate independently and hence,  $p_c$  can be modelled as being sampled from a distribution  $f(p_c)$ , bounded between  $p_{c,\text{min}}$  and  $p_{c,\text{max}}$ . The mean cyclic hypoxic fraction is thus given by

$$\langle \text{HF}_{\text{cyclic}} \rangle = \int_{p_{c,\text{min}}}^{p_{c,\text{max}}} f(p_c) \text{HF}_{\Lambda}(p_c) dp_c - \text{HF}_{\Lambda}(p_{c,\text{max}}). \quad (5)$$

Owing to the differing time scales involved, the potential cyclic hypoxic fraction will play a role in our (brief) discussion of hypoxia binding agents (e.g., pimonidazole and those used in positron-emission tomography imaging of hypoxia), while the mean cyclic hypoxic fraction arises in our model of radiotherapy response.

The above definitions are completely general. As a specific model of the microscopic hypoxic fraction, consider a randomly distributed vasculature, shown schematically in Fig. 1(a.). Oxygen diffuses a characteristic distance  $l_D \equiv \sqrt{4D_{\text{O}_2}p_c/M}$  from each capillary before being completely consumed<sup>32</sup>. Here,  $D_{\text{O}_2}$  is the diffusivity of oxygen and  $M$  is the oxygen consumption rate (mmHg/s, for  $p_c$  expressed in mmHg). In a “micro-region” of tissue in which these quantities are very nearly constant, the fraction of tissue that is at nearly zero oxygen tension is thus approximated by Poisson statistics:

$$\text{HF}_{\Lambda}(p_c) \sim e^{-\pi n_c l_D^2} \equiv e^{-\gamma n_c}, \quad \gamma \equiv \frac{4\pi D_{\text{O}_2} p_c}{M}, \quad (6)$$

where  $n_c$  is the areal capillary density (number of capillaries per unit area in a given tissue plane) in the pseudo-voxel in question. Equation (6) is an approximation to the solution of the oxygen reaction-diffusion equation with randomly distributed capillaries acting as

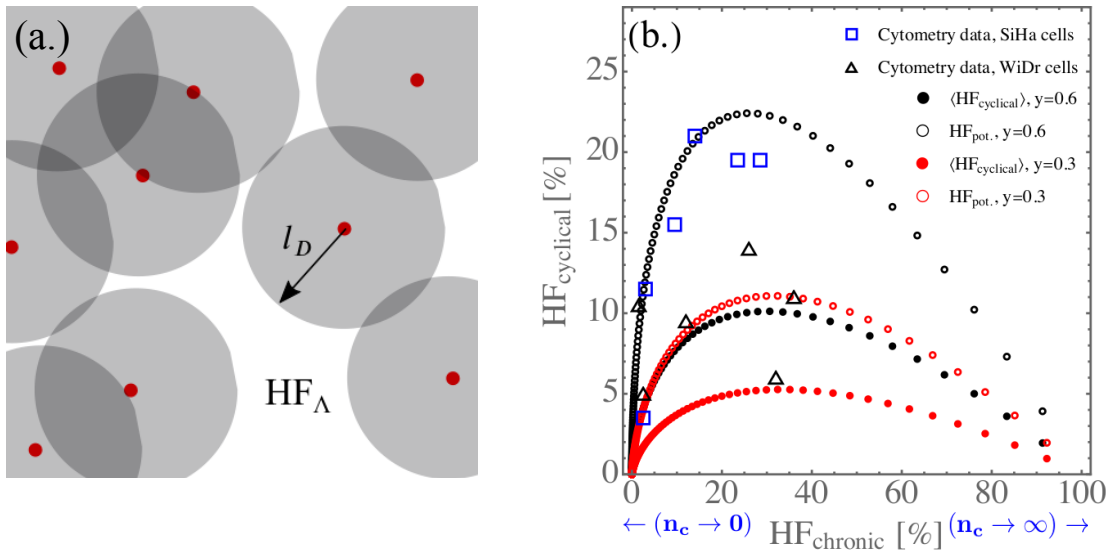


Figure 1: (a.) Graphical representation of the model shown in Eq. (6). Oxygen diffuses a characteristic distance  $l_D$  from capillaries, leaving a fraction  $HF_{\Lambda}$  of tissue hypoxic (unshaded region). For randomly distributed capillaries, this fraction is given by Poisson statistics:  $\exp(-\pi n_c l_D^2)$ . (b.) Potential cyclical and mean cyclical versus chronic hypoxia, obtained from Eqs. (8-10) for two representative values of the oxygen fluctuation parameter  $y \equiv (\Delta p_c / \bar{p}_c) = 0.3$  and  $0.6$ . Also shown is flow cytometry data for two cell lines, extracted from Figs. 2 and 5 of Bennewith and Durand<sup>10</sup> (see text for details). The left and right sides of this plot correspond to the hypo- ( $n_c \rightarrow 0$ ) and well-perfused ( $n_c \rightarrow \infty$ ) limits, respectively.

oxygen sources<sup>27,33</sup>. It is approximate since it treats the oxygen “fields” [the shaded circles in Fig. 1(a.)] emanating from each capillary as independent of each other. In dealing with the distance  $l_D$  from a capillary required for the oxygen tension to vanish, Eq. (6) also implicitly assumes that  $\Lambda = 0$ ; formally, nonzero  $\Lambda$  can be accounted for by correcting the diffusion distance:  $l_D \rightarrow l_D(1 - \Lambda/p_c)$ . We will ignore this small correction and continue to treat  $\Lambda$  as small ( $\lesssim 5$  mmHg), but nonzero.

Cyclic and chronic hypoxia are not independent but are connected by the vascular architecture and capillary oxygen tension kinetics: for a given rate of oxygen metabolism  $M$ , both the chronic and cyclic hypoxic fractions are functions of the capillary density and the amplitude  $\Delta p_c \equiv p_{c,\max} - p_{c,\min}$  of capillary oxygen tension fluctuations. Thus, chronic and cyclic hypoxia go hand-in-hand, primarily functions of the underlying tissue capillary

density. Choosing for simplicity a uniform, “top-hat” function

$$f(p_c) = \begin{cases} 1/\Delta p_c & \text{for } p_{c,\min} \leq p_c \leq p_{c,\max} \\ 0 & \text{otherwise} \end{cases} \quad (7)$$

to represent the distribution of capillary oxygen fluctuations in Eqs. (3-5) gives

$$\text{HF}_{\text{chronic}} = e^{-x} e^{-z/2}, \quad (8)$$

$$\text{HF}_{\text{pot.}} = 2e^{-x} \sinh(z/2), \quad (9)$$

and

$$\langle \text{HF}_{\text{cyclic}} \rangle = e^{-x} \frac{\sinh(z/2)}{(z/2)} - \text{HF}_{\text{chronic}}. \quad (10)$$

Here, we have defined the dimensionless parameters

$$x \equiv \bar{\gamma} n_c, \quad y \equiv \left( \frac{\Delta p_c}{\bar{p}_c} \right), \quad \text{and} \quad z \equiv x \cdot y, \quad (11)$$

with  $\bar{p}_c$  is the mean capillary oxygen tension, and  $\bar{\gamma} \equiv 4\pi D_{\text{O}_2} \bar{p}_c / M$  the mean  $\gamma$  value. These parameters are the key variables regulating the magnitude of cyclic hypoxia and its impact on radiotherapy.  $x$  describes the efficiency with which the vasculature delivers oxygen: when  $x \lesssim 1$ , the mean distance  $l_D$  travelled by oxygen from capillaries is shorter than the mean distance  $\sim 1/\sqrt{n_c}$  between capillaries, and oxygen does not reach all tissue, resulting in substantial  $\text{HF}_{\text{chronic}}$ . In the opposite regime where,  $x \gtrsim 1$ , tissue is well-perfused and the chronic hypoxic fraction is small.  $y$  quantifies the amplitude of capillary oxygen tension fluctuations. In the limit  $y \rightarrow 0$  that oxygen tension fluctuations vanish, both terms on the right-hand side of Eq. (10) reduce to  $\exp(-x)$  and hence,  $\langle \text{HF}_{\text{cyclic}} \rangle$  vanishes.  $z$  is a compound parameter describing both the amplitude of capillary oxygen fluctuations as well as the baseline vascular oxygen deliver efficiency and hence, characterizes the magnitude of tissue oxygen fluctuations that result from fluctuations in capillary tension.

Any reasonable alternative choice (e.g., log-normal) for the distribution function shown in Eq. (7) would yield qualitatively similar results to ours here. We chose the top-hat form since, in addition to yielding analytic results for the hypoxic fractions and survival fractions following RT, it minimizes the number of parameters in our model.

## I.A. Hypoxia model parameter values

Using the classic value  $l_D \sim 150 \mu\text{m}$  derived by Thomlinson and Gray<sup>32</sup>, we estimate  $\bar{\gamma} = 7 \times 10^{-2} \text{ mm}^2$ . In arriving at this value for  $l_D$ , these authors also assumed  $\bar{p}_c \sim 40 \text{ mmHg}$ ,

the value we adopt here as well. Estimates of the capillary density  $n_c$  vary widely<sup>34,35,36,37,38</sup>, with typical values spanning  $(5 - 500) \text{ mm}^{-2}$ . Thus,  $x \equiv \bar{\gamma}n_c$  varies from  $\sim 0.1$  to  $\sim 10$ . Note that vessel quantification studies such as these measure the “microvascular density” and do not distinguish capillaries from small arterioles and venules. Thus, these values may overestimate  $n_c$ . Measurements of vascular and peri-vascular oxygen tension fluctuations reveal maximum amplitudes  $\Delta p_c$  on the order of  $(5 - 25) \text{ mmHg}$ <sup>8,9</sup> and hence,  $y \equiv \Delta p_c/\bar{p}_c$  varies from  $\sim 0.1$  to  $\sim 0.6$ . For some context, using the representative value  $y = 0.4$ , for  $x = 0.1$  (poorly-perfused tissue),  $\text{HF}_{\text{chronic}} \sim 0.9$  and  $\langle \text{HF}_{\text{cyclic}} \rangle \sim 10^{-2}$ , while for  $x = 10$  (well-perfused),  $\text{HF}_{\text{chronic}} \sim 10^{-5}$  and  $\langle \text{HF}_{\text{cyclic}} \rangle \sim 10^{-4}$ .

In Figure 1(b.), we plot  $\langle \text{HF}_{\text{cyclic}} \rangle$  and  $\text{HF}_{\text{pot.}}$  as functions of  $\text{HF}_{\text{chronic}}$ , using  $y = 0.6$  and  $y = 0.3$  as illustrative values. In the same plot, we show the cyclic and chronic hypoxic fractions estimated from flow cytometry data acquired by Bennewith and Durand<sup>10</sup> from xenografts exposed to two different hypoxia markers (pimonidazole and CCI-103F) for different durations to distinguish these fractions. The data points shown in this plot were extracted from individual bins for each xenograft–human cervical (SiHa) and colon (WiDr) cancers–, representing different intensities for the fluorescent perfusion dye Hoechst 33342. This way, each datapoint shown in Fig. 1(b.) represents a different distance bin from nearest capillaries. As long as the time  $T$  that these tracers spend in the blood is greater than several periods of cyclic hypoxia fluctuations, markers such as these serve as “integral” ones, labelling all cells that were hypoxic at some point during  $T$  and hence, the uptake will be proportional to  $\text{HF}_{\text{pot.}}$ , and not  $\langle \text{HF}_{\text{cyclic}} \rangle$ . We make no attempt to fit this data to our model, but present it here to give an idea of the magnitudes of measured transient and chronic hypoxias. However, we note two properties that our model curves shown in this plot possess that any physiologically valid model as well as empirical data must satisfy: in the completely avascular limit,  $n_c \rightarrow 0$ , any fluctuations in capillary oxygen tension hypoxia will not impact tissue oxygen levels, which remain identically zero:  $\text{HF}_{\text{chronic}} \rightarrow 1$  and  $\langle \text{HF}_{\text{cyclic}} \rangle \rightarrow 0$ . In the opposite limit, of well-vascularized tissue,  $n_c \rightarrow \infty$  (in practice, for our parameter choices,  $n_c \gtrsim 100 \text{ mm}^{-2}$  suffices), fluctuations in  $p_c$  likewise have no impact on the completely oxic tissue:  $\text{HF}_{\text{chronic}} \rightarrow 0$  and  $\langle \text{HF}_{\text{cyclic}} \rangle \rightarrow 0$ . Hence, the exact  $\langle \text{HF}_{\text{cyclic}} \rangle$  versus  $\text{HF}_{\text{chronic}}$  relationship must have the general shape shown in Fig. 1(b.).

## II. Cyclic hypoxia and clonogen survival fraction during hypofractionated radiotherapy

Having introduced our model for cyclic hypoxia [Eqs. (8-10)], we now turn to the problem of working out its impact on RT response. Consistent with the discussion in the Introduction, the surviving fraction  $SF^{(1)}$  of cancer clonogens after a single fraction of radiotherapy is approximated as

$$SF^{(1)} \simeq \langle HF_{\text{cyclic}} \rangle \cdot SF_{\text{cyclic}} + HF_{\text{chronic}} \cdot SF_{\text{chronic}} + (1 - \langle HF_{\text{cyclic}} \rangle - HF_{\text{chronic}}) \cdot SF_{\text{oxic}}, \quad (12)$$

where the survival fractions in each compartment are given by Eq. (1). This expression extends the binary decomposition used by Carlson *et al.*<sup>20</sup> to include both chronic and cyclic hypoxia compartments, in addition to an oxic one. In reality, the survival fraction is given by a convolution over a continuous spectrum of oxygen tensions<sup>15,27</sup>. The rapid variation of the OER with respect to oxygen tension at low values ( $\lesssim 5$  mmHg)<sup>1</sup> justifies the compartmentalization in Eq. (12); however, this approximation can lead to quantitative errors in  $SF^{(1)}$ .

Neglecting proliferation during abbreviated hypofractionated treatments and assuming that there is no reoxygenation, for us meaning that  $\langle HF_{\text{cyclic}} \rangle$  and  $HF_{\text{chronic}}$  remain constant through treatment, the survival fraction after  $N$  fractions is approximated as

$$SF^{(N)} \simeq \sum_{m=0}^N P(m, N-m) (SF_{\text{cyclic}})^m (SF_{\text{oxic}})^{N-m} + HF_{\text{chronic}} \cdot (SF_{\text{chronic}})^N. \quad (13)$$

Here,  $P(m, N-m)$  is the probability that a non-chronically hypoxic cell is hypoxic for  $m$  fractions, and oxic for the remaining  $N-m$ . Because it excludes the chronically hypoxic population [accounted for in the last term in Eq. (13)], it satisfies the normalization condition  $\sum_{m=0}^N P(m, N-m) = 1 - HF_{\text{chronic}}$ . For a single fraction ( $N = 1$ ), this probability is simply the mean cyclic hypoxic fraction,

$$P(1, 0) = \langle HF_{\text{cyclic}} \rangle \quad (14)$$

and hence, Eq. (13) reduces to Eq. (12) when  $N = 1$ .

As noted in the Introduction, for hypofractionated RT regimens, the survival fractions in the oxic and even chronically hypoxic compartments are parametrically smaller than that

for the cyclically hypoxic one. Thus, absent reoxygenation, the surviving clonogens will be those in the cyclically hypoxic compartment that remain cyclically hypoxic for the duration of treatment:

$$\text{SF}^{(N)} \simeq P(N, 0)(\text{SF}_{\text{cyclic}})^N. \quad (15)$$

It thus remains to derive an expression for  $P(N, 0)$  to estimate the impact of fractionation on a tumour with a cyclically hypoxic population.

Consider a pseudo-voxel for which the capillary oxygen tensions through  $N$  fractions of radiotherapy are  $p_c^{(1)}, p_c^{(2)}, \dots, p_c^{(N)}$ . Assuming that the vasculature remains constant over the  $N$  fractions, the fraction  $p(N, 0)$  of non-chronically hypoxic tissue in this pseudo-voxel that remains hypoxic for all  $N$  fractions is

$$p(N, 0) = \text{HF}_{\Lambda}(\max[p_c]) - \text{HF}_{\text{chronic}}, \quad (16)$$

where  $\max[p_c]$  is the maximum of the  $p_c^{(1)}, p_c^{(2)}, \dots, p_c^{(N)}$  values. Note that this is not in general equal to  $p_{c,\text{max}}$ , but is bounded from above by it. Although high doses per fraction ( $\gtrsim 8$  Gy) can ablate the vasculature<sup>39,40</sup>, substantial ( $\gtrsim 20\%$ ) losses do not occur until after 1-2 weeks<sup>40</sup>, justifying our approximation of a constant vasculature over the hypofractionated schedules of interest to us here.

Generalizing the result shown in Eq. (16) to average over all possible realizations of sequences of  $p_c$  values [sampled from the distribution  $f(p_c)$ ] by defining  $P(N, 0) \equiv \langle p(N, 0) \rangle$ , gives

$$P(N, 0) = N \int_0^\infty dp_c^{(1)} f(p_c^{(1)}) \text{HF}_{\Lambda}(p_c^{(1)}) \left\{ \int_0^\infty dp_c^{(2)} f(p_c^{(2)}) \Theta(p_c^{(1)} - p_c^{(2)}) \times \right. \\ \left. \dots \times \int_0^\infty dp_c^{(N)} f(p_c^{(N)}) \Theta(p_c^{(1)} - p_c^{(N)}) \right\} - \text{HF}_{\text{chronic}}. \quad (17)$$

The factor  $N$  in front of the integrals arises since we have arbitrarily chosen  $p_c^{(1)}$  to be the maximum value of  $p_c$ , as enforced by the Heaviside theta functions  $\Theta$ , and there were  $N$  choices for the fraction with the maximum  $p_c$  value.

Using Eq. (7) in Eq. (17), the resulting integral can be evaluated analytically, with the result

$$P(N, 0) = \langle \text{HF}_{\text{cyclic}} \rangle \cdot F(z, N) - \text{HF}_{\text{chronic}} \cdot [1 - F(z, N)], \quad (18)$$

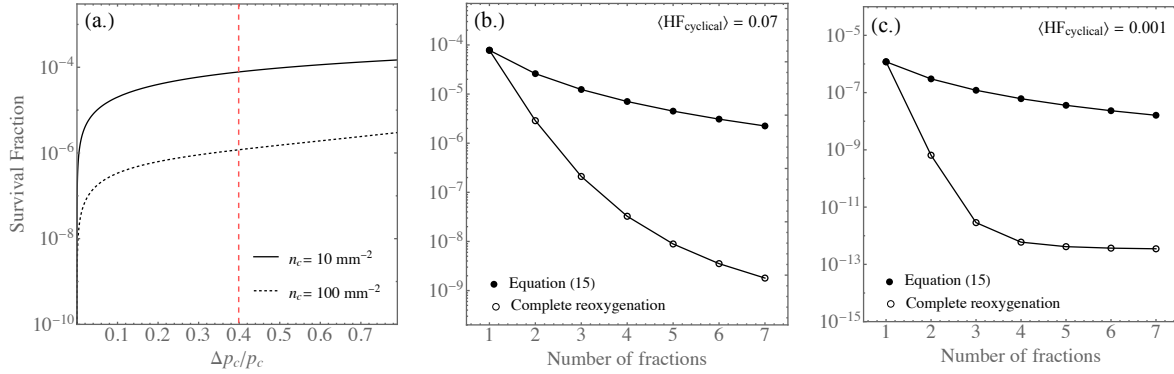


Figure 2: Clonogen survival fraction versus (a.) the amplitude  $y \equiv (\Delta p_c/\bar{p}_c)$  of capillary oxygen partial pressure fluctuations and (b.), (c.) number of fractions for iso-BED schedules (relative to 60 Gy in 30 fractions, with  $\alpha/\beta = 10$ ). The dashed-vertical line in (a.) indicates  $y = 0.4$ , the representative value used in the remainder of this manuscript. In (b.) and (c.), SF is shown using this value and  $n_c = 10$  and  $100 \text{ mm}^{-2}$ , respectively. Also shown in these plots are the survival fractions assuming complete reoxygenation, given by Eq. (21). For all panels,  $\alpha = 0.4 \text{ Gy}^{-1}$  and  $\alpha/\beta = 10 \text{ Gy}$ .

where

$$F(z, N) \equiv \frac{N [\Gamma(N) - \Gamma(N, z)]}{z^{N-1} (1 - e^{-z})}. \quad (19)$$

Here,  $\Gamma(N)$  and  $\Gamma(N, z)$  are the complete and incomplete Euler gamma functions, respectively. It can be shown that  $F(z, 1) = 1 \forall z$  and hence, Eq. (14) is recovered. For nonzero  $z$ ,  $F(z, N)$  decreases with increasing number  $N$  of fractions, reflecting the increase in clonogen cell-killing (decrease in SF) due to inter-fraction oxygen fluctuations. To express this effect in terms of biologically effective doses, we define an iso-survival fraction BED as:

$$\begin{aligned} \text{BED}_{\text{iso-SF}}(N) &\equiv -\frac{1}{\alpha} \ln(\text{SF}^{(N)}) = \frac{Nd}{\text{OER}_{\text{cyclic}}} \left( 1 + \frac{d}{(\alpha/\beta)\text{OER}_{\text{cyclic}}} \right) + \frac{1}{\alpha} \ln[P^{-1}(N, 0)] \\ &\equiv \text{BED}_{\text{cyclic}}(N) + \frac{1}{\alpha} \ln[P^{-1}(N, 0)]. \end{aligned} \quad (20)$$

When  $N = 1$ ,  $F(z, 1) = 1$  and the iso-SF BED for the hypoxic fraction reduces to  $\text{BED}_{\text{cyclic}}$ . When  $N > 1$ , the second term on the right-hand side is non-zero and positive; it represents the added BED arising from inter-fraction fluctuations in oxygen levels.

Taken together, Eqs. (15), (18), and (20) constitute the primary results of this manuscript. They quantify the impact of cyclic hypoxia on hypofractionated radiotherapy treatments via the estimated fraction of surviving clonogens and the dose needed to

counteract the loss of cell-killing due to the reduction in oxygen fluctuations with fewer fractions. The key parameters governing this impact are the fractionation regimen ( $d$ ,  $N$ ) and the compound parameter  $z$ , which multiplies the vasculature efficiency parameter  $x$  and the amplitude  $y$  of capillary oxygen fluctuations; see Eq. (11). In Figure 2, using  $\alpha = 0.4 \text{ Gy}^{-1}$  and  $\alpha/\beta = 10 \text{ Gy}$ , we plot SF as a function of (a.) the amplitude  $y$  of capillary oxygen fluctuations and (b.)-(c.), the number of fractions for nominally iso-BED doses. From Fig. 2(a.), it can be seen that, except for very small values of  $y$ , SF increases slowly with  $y$  and we use  $y = 0.4$  for the remainder of the results in this manuscript, noting the weak dependence of our results on this parameter. Survival fractions in Figs. 2(b.) and 2(c.) are plotted as functions of the number of fractions, iso-BED with (the arbitrarily chosen conventional RT schedule 60 Gy in 30 fractions), for two representative values of the capillary density,  $n_c = 10$  and  $100 \text{ mm}^{-2}$ . Respectively, these correspond to  $x = 0.7$  and  $7$  (poorly- and well-perfused tumours) and cyclic (chronic) hypoxic fractions of  $0.07(0.43)$  and  $0.001(0.0002)$ . By “iso-BED”, we mean in the usual sense of iso-BED<sub>oxic</sub>; that is, neglecting OER corrections (by setting OER = 1) in Eq. (2). For  $N = 1$ , for instance, using  $\alpha/\beta = 10$ , the iso-BED (to 60 Gy in 30) dose is 22.3 Gy. The value  $\alpha \simeq 0.4 \text{ Gy}^{-1}$  used in these plots is a commonly used value in theoretical radiobiological studies of e.g., head and neck tumours<sup>15</sup>, while also being consistent with radiobiological studies of lung cancers<sup>25</sup>.  $\alpha/\beta = 10 \text{ Gy}$  is a standard value for early-responding (non-prostate) tumour tissues. Also shown in Figure 2(b.) and (c.) are the survival fractions when complete, *stochastic* reoxygenation is assumed, corresponding to<sup>20</sup>

$$\text{SF}^{(N)} = (\text{SF}^{(1)})^N, \text{ complete reoxygenation.} \quad (21)$$

Figure 2 shows that cyclic hypoxia enhances the efficacy of nominally iso-BED (iso-BED<sub>oxic</sub>) radiotherapy with increasing number of fractions, a result of tissue that is initially hypoxic becoming oxic at subsequent fractions due to transient fluctuations. For e.g.,  $\langle \text{HF}_{\text{cyclic}} \rangle = 0.07$  [shown in Fig. 2(b.)], clonogen cell survival increases by approximately a factor 30 in going from five fractions to a single one. Although SF increases with decreasing fraction number, the increase is much smaller than arises when complete stochastic reoxygenation occurs between fractions. In the same figure, the assumption of complete reoxygenation leads to a *much* larger increase in SF, by a factor  $\sim 10^5$ .

The expression for the iso-survival fraction biologically effective dose, Eq. (20), gives a

convenient way of comparing the efficacy of different fractionation schedules.  $\text{BED}_{\text{iso-SF}}$ 's for some common SBRT fractionations schedules are presented in Sec. III.

### III. Discussion

Driven by advances in technology that have allowed for the reliable delivery of more conformal dose distributions, the use of hypofractionated treatments such as SBRT has grown considerably over the past two decades. Although SBRT has clear efficiency benefits, *prima facie*, it is likely suboptimal radiobiologically. Setting aside the differential repair of sub-lethal DNA damage between early- and late-responding tissues, SBRT challenges two of the “4 R’s of radiotherapy”<sup>41</sup>: reoxygenation and redistribution through the cell cycle, which enhance radiosensitivity over time. The impact of hypofractionated radiotherapy regimens on tumours with hypoxia has been widely discussed<sup>18,20,24,26,42,43</sup>, and the general conclusion has been that tumour control probability will be reduced with fewer fractions because of the reduced extent of reoxygenation. Why has hypofractionated radiotherapy been so successful then, with no clear evidence of plunging control probabilities even for single-fraction regimens<sup>42,44</sup>?

Based on our results, we give two potential reasons for this: first, assuming that reoxygenation does not occur to a substantial degree during hypofractionated RT, cyclic hypoxia was found to result in a more modest decrease in clonogen survival with decreasing fractionation, as compared to models that assume a complete “stochastic” reoxygenation; see Fig. 2. Second, as we discuss below, in sites such as pancreas and lung, increasing hypofractionation has been accompanied by increasing BED’s, largely offsetting the smaller increase in survival predicted here.

“Complete reoxygenation” conventionally refers to the phenomenon wherein the hypoxic fraction of *viable* cells (i.e., slated for death but possibly still intact and metabolising) remains approximately constant at each fraction<sup>45</sup>. Further assuming that cells are randomly reassigned to this hypoxic compartment (i.e., stochastic reoxygenation, with probability equal to the hypoxic fraction) at each fraction leads to the result shown in Eq. (21). As was noted in the Introduction, this widely-used approximation likely overestimates the effect of hypofractionation, since it neglects to take into account that the oxygen level kinetics of a

Biologically effective doses for some common SBRT regimens				
Site	$D, N$	$\text{BED}_{\text{oxic}}$	$\text{BED}_{\text{iso-SF}}$ ( $n_c = 10 \text{ mm}^{-2}$ )	$\text{BED}_{\text{iso-SF}}$ ( $n_c = 100 \text{ mm}^{-2}$ )
Lung	50, 5 <sup>46</sup>	100	38	50
	48, 4 <sup>47</sup>	106	38	49
	34, 1 <sup>47</sup>	150	39	49
	27*, 1 <sup>48</sup>	100	29	40
Pancreas	40-50, 5 <sup>49,50</sup>	72-100	31-38	43-50
	36, 3 <sup>51</sup>	79	30	42
	25, 1 <sup>52</sup>	88	27	37
Liver	35-40, 5 <sup>53,54</sup>	60-72	29-32	43-46
	40-48, 3 <sup>55,56</sup>	93-125	34-41	48-55
Prostate	42.7, 7 <sup>57</sup>	130	59	105
	36.25, 5 <sup>58</sup>	124	54	100
	19, 1 <sup>59</sup>	139	45	84

Table 1: Biologically effective doses for some common SBRT schedules, described by the total dose  $D \equiv Nd$  and number of fractions,  $N$ . Lung cancer and liver schedules refer to early-stage non-small-cell and primary liver cancers, respectively. All BED's are expressed in units of  $\text{Gy}_{\alpha/\beta}$ . For non-prostate sites,  $\alpha = 0.4 \text{ Gy}^{-1}$  and  $\alpha/\beta = 10 \text{ Gy}$  were used; for prostate, we used  $\alpha = 0.15 \text{ Gy}^{-1}$  and  $\alpha/\beta = 3 \text{ Gy}$ <sup>60</sup>. Iso-SF BED's [Eq. (20)] are shown for two representative capillary densities and were calculated using  $y = 0.4$ . \*Estimated dose accounting for tissue heterogeneity corrections.

given cell depends on its proximity to the nearest capillary and is *not* stochastic. In our model, a cell in close proximity to a blood vessel [i.e., the population of cells not described by Eq. (6)] would remain oxic even when the capillary oxygen tension reaches its minimum value (as long as  $p_{c,\min} > 0$ ; i.e.,  $y < 1$ ). Mathematically, this lack of stochasticity is manifested as  $P(N, 0) \gg [P(1, 0)]^N$  being well-satisfied for  $N > 1$ ; that is, the probability that a (non-chronically hypoxic) clonogen will be hypoxic for all  $N$  fractions is much greater than  $\langle \text{HF}_{\text{cyclic}} \rangle^N$ . Hence, the decay in cell-killing with decreasing fractionation is much lower than would occur for completely stochastic dynamics.

Even though our model predicts a much smaller reduction in SF, a 1-2 log increase in SF [e.g., Fig. 2(b.)] in going from  $\sim$ five to one fraction would likely have observable clinical effects except for the fact that, for the most part, hypofractionation has been accompanied by increases in doses and are not “iso-BED” ( $\text{iso-BED}_{\text{oxic}}$ ). This is apparent in Table 1, where we list the biologically effective doses— $\text{BED}_{\text{oxic}}$  and  $\text{BED}_{\text{iso-SF}}$  for two representative values

of the capillary density—for some common SBRT regimens. As an example, for early-stage non-small cell lung cancers, in going from 50 Gy in five fractions<sup>46</sup> to 34 Gy in a single fraction (RTOG 0915<sup>47</sup>),  $\text{BED}_{\text{oxic}}$  increased from  $100 \text{ Gy}_{10}$  to  $150 \text{ Gy}_{10}$ . At the same time, the iso-SF BED's defined in Eq. (20) are nearly identical, reflecting the fact that the  $50 \text{ Gy}_{10}$  increase in  $\text{BED}_{\text{oxic}}$  was just enough to overcome the loss of cell killing due to the diminished effect of inter-fraction oxygen fluctuations.

Although  $\text{BED}_{\text{iso-SF}}$  depends sensitively on the capillary density  $n_c$ , the relative  $\text{BED}_{\text{iso-SF}}$  between different fractions remains largely unchanged. It is also interesting that survival fractions were not overly sensitive to the precise value of the amplitude  $y$  of capillary oxygen tension fluctuations [Fig. 2(a.)], meaning that almost any (non-zero) degree of cyclic hypoxia would produce comparable  $\text{BED}_{\text{iso-SF}}$ 's. Together, these suggest that  $\text{BED}_{\text{iso-SF}}$  could be used to compare fractionation schedules, even without knowing  $n_c$  or  $\Delta p_c$  precisely.

For most three-to-five fraction regimens in lung, liver, and pancreatic cancers, the estimated iso-SF BED's are nearly the same, providing a possible explanation for why extreme hypofractionation seems to have largely been a success<sup>42,44,47</sup>. Primary liver disease is a particularly interesting case, given the apparent absence of a strong dose-response relationship<sup>61</sup>. Even though this is undoubtedly due in part to the high rates of local control (LC) in this disease site<sup>62</sup>, it is still surprising that even a factor three increase in the nominal BED ( $\text{BED}_{\text{oxic}}$ ) has such little apparent effect on LC. Accounting for cyclic hypoxia, however, the spread in the iso-SF BED's is greatly reduced, from three to a factor of  $\sim 1.4$ .

Nonetheless, our analysis suggests that care should be taken with single-fraction regimens, in particular lung 27 Gy<sup>48</sup> and prostate 19 Gy<sup>59</sup> regimens may be under-dosing tumours when factoring in the impact of cyclic hypoxia. Local control rates and survival at two years have been reported for the lung study and are similar to those in comparable few-fraction regimens<sup>48</sup>. It is unlikely, however, that a 1-2 log difference in cell survival would result in a substantial difference in these metrics at two years post-treatment. As an example of this, consider a poorly-perfused lung tumour with  $x = 0.7$  ( $\langle \text{HF}_{\text{cyclic}} \rangle = 0.07$ ). Using Eq. (15), the SF is estimated to be  $3 \times 10^{-9}$  and  $1 \times 10^{-7}$  for 48 Gy in four fractions and 27 Gy in a single fraction, respectively. Now, assuming that some clonogens survived treatment and a tumour doubling time  $\tau_d$  of 100 days<sup>25</sup>, it would take  $\sim 6$  and  $\sim 4$  years ( $= -\tau_d \cdot \ln(\text{SF}) / \ln 2$ ), respectively, for the tumours to regrow to their pre-SBRT sizes. As-

sessments of treatment response efficacy should thus only be made at least four years after completion of SBRT in sites with high rates of control. Another example is provided by monotherapy prostate brachytherapy, where 19 Gy in a single fraction was found to be inferior to (the iso-BED<sub>oxic</sub> schedule) 27 Gy in two fractions, a difference that was only clearly apparent *after* several years of follow-up<sup>63</sup>.

Our estimates of clonogen survival and the resulting iso-SF BED are dependent on a number of approximations. The accuracy of the linear quadratic model [Eqs. (1) and (2)] has been questioned for high doses per fraction<sup>64</sup>. In assessing clinical data, however, others have argued that there is no discernible breakdown of the LQ model<sup>65</sup>, in particular when accounting for heterogeneous oxygen distributions that arise in tumours<sup>25,66</sup>. As we have noted throughout this manuscript, the spatial relationship between hypoxia and the vasculature plays a key role in determining the impact of cyclic hypoxia on radiation response since it is responsible for the non-stochasticity of regional levels of hypoxia going through treatment. Our simple expression for this spatial relationship—given by Eq. (6)—as well as the compartmentalization used in Eqs. (13) and (15), are approximations to the continuum distribution of oxygen, obtained by solving the oxygen reaction-diffusion equation for simulated capillary architectures<sup>22,30</sup>. We believe, however, that our model captures the essence of cyclic hypoxia and its impact on hypofractionation and that its simplicity will facilitate analyses of SBRT response, in particular for sites where functional imaging is available to assess hypoxia and perfusion.

In addition to solving the full reaction-diffusion equations in their study of cyclic hypoxia and hypofractionated RT, Lindblom and collaborators modelled cyclic hypoxia as a transient, localized occlusion of blood vessels<sup>22</sup>. Although there is significant evidence indicates that this is not the case, and that cyclic hypoxia is caused by transient fluctuations in perfusion<sup>8,9,31</sup>, this distinction would not qualitatively change the results of our study or the work of Lindblom *et al.* It would still be the case that cells proximal to capillaries are less likely to find themselves hypoxic at different fractions. Both studies thus find that the impact of hypofractionation is less than would be expected based on the assumption of complete, stochastic, reoxygenation.

The final major assumption made by us in this work is that substantial reoxygenation (stochastic or otherwise) does not take place during hypofractionated RT. A large body

of work has investigated reoxygenation and two types of reoxygenation can be discerned: 1.) transient reoxygenation, occurring up to several hours after radiation, due to transient metabolic or perfusion changes<sup>67,68</sup> and 2.) “long-term” ( $\gtrsim 1$  week) reoxygenation kinetics, arising from a reduction in metabolic capacity due to cell death<sup>25</sup> and the lysing kinetics of cells killed by RT resulting in blood vessels being brought closer to previously hypoxic cells<sup>45</sup>. Both these sources of reoxygenation are unlikely to have a large impact on hypofractionated treatments lasting  $\sim 1$  week, with fractions separated by a day or more. Consistent with this, recent pre-clinical measurements of hypoxia using positron-emission tomography in pancreatic tumours revealed only a modest amount of reoxygenation over five fractions (delivered every second day, with hypoxia measurements separated by two weeks)<sup>17</sup>. Additionally, Kaleda and colleagues found *increased* levels of hypoxia after (2-4 days post RT) large-dose single-fraction radiotherapy in lung tumours<sup>69</sup>.

A limitation of the present work is that we have only compared different ultra-hypofractionated radiotherapy regimens with each other, and not with conventionally fractionated regimens. To do so would require modelling reoxygenation<sup>25,26</sup>, as well as using the more general expression for survival fraction given by Eq. (13) and hence, computation of  $P(m, N - m)$  for  $m \neq N$ , since these probabilities become non-negligible for smaller per-fraction doses. These straightforward generalizations will be considered in future work.

In closing, let us ask: are there any actionable discoveries here? Motivated by a desire to understand the apparent success of ultra-hypofractionated radiotherapy regimens, we showed that most of these regimens increase dose sufficiently with decreasing fraction number to overcome the increase in clonogen survival arising from the loss of inter-fraction oxygen fluctuations. Can we offer any recommendations for improvements, then? One possibility concerns “dose painting”, the delivery of higher doses to more hypoxic regions, typically quantified by positron-emission tomography (PET) using specialized hypoxia-sensitive tracers<sup>15,27,70,71,72</sup>. As with pimonidazole (discussed in Sec. I.A.), these tracers are integral markers of cyclic hypoxia, and tracer uptake in cyclically hypoxic cells will be correspondingly smaller than that in chronically hypoxic ones<sup>73</sup>. Because chronically hypoxic cells are also less radioresistant than cyclically hypoxic ones, the survival fraction versus uptake curve (needed for dose painting<sup>27</sup>) is relatively “flat”, restricting the opportunity to meaningfully dose paint based on PET signal. In contrast, our model predicts that the SF versus capillary density ( $n_c$ ) curve will be sharply peaked, reflecting the fact that most radioresistant cycli-

cally hypoxic cells lie in the middle ground between very well-perfused and hypo-perfused; see the right panel of Fig. 1. This suggests that patients may benefit from dose painting based on *perfusion* measurements. For our chosen parameter values, SF is maximal for  $n_c \sim 10 \text{ mm}^{-2}$  and is decreased by a factor  $\sim 10^2$  in going to  $n_c \sim 100 \text{ mm}^{-2}$ , encompassing a typical range measured in solid tumours<sup>35,37,38</sup>. Thus, delivery of higher doses to regions with lower  $n_c$  (but not  $\lesssim 10 \text{ mm}^{-2}$ ) would decrease clonogen survival. Apart from the inability of hypoxia-PET imaging to resolve cyclic and chronic hypoxia, an advantage of this approach over PET imaging is that qualitative perfusion measurements (e.g., biphasic imaging for liver and pancreatic cancers) are part of routine clinical practice and moreover, even qualitative<sup>74</sup> and semi-quantitative<sup>75</sup> metrics have been shown to correlate with microvascular density. Although the precise parameter values (e.g., the rate of oxygen metabolism) required to derive the patient-specific SF versus  $n_c$  curve are unknown, the preponderance of perfusion imaging means that it should be possible to derive empirical population-averaged curves<sup>76,77</sup> by integrating perfusion images with dose distribution maps and outcome data.

## IV. Conclusions

Cells that are transiently hypoxic are approximately twice as radioresistant as chronically hypoxic cells and between two and three times more radioresistant than oxic cells and hence, the kinetics of this population through hypofractionated radiotherapy plays a major role in determining treatment response. Using simple analytic approximations for the spatial-temporal dynamics of cyclic hypoxia, we estimated that most ultra-hypofractionated regimens give enough dose to counter losses in clonogen cell-killing with increasing hypofractionation, although some lung and prostate single-fraction regimens may be under-dosing tumours. Dose painting based on perfusion imaging may provide a way to target the cyclically hypoxic population.

## References

- <sup>1</sup> T. Alper and P. Howard-Flanders, Role of Oxygen in Modifying the Radiosensitivity of E. Coli B., *Nature* **178**, 978–979 (1956).
- <sup>2</sup> B. G. Wouters and J. M. Brown, Cells at Intermediate Oxygen Levels Can Be More Im-

portant Than the "Hypoxic Fraction" in Determining Tumor Response to Fractionated Radiotherapy, *Radiation Research* **147**, 541 (1997).

<sup>3</sup> R. P. Hill, R. G. Bristow, A. Fyles, M. Koritzinsky, M. Milosevic, and B. G. Wouters, Hypoxia and Predicting Radiation Response, *Seminars in Radiation Oncology* **25**, 260 – 272 (2015).

<sup>4</sup> J. M. Brown, Evidence for acutely hypoxic cells in mouse tumours, and a possible mechanism of reoxygenation, *The British Journal of Radiology* **52**, 650–656 (1979).

<sup>5</sup> H. Yamaura and T. Matsuzawa, Tumour Regrowth after Irradiation, *International Journal of Radiation Biology and Related Studies in Physics, Chemistry and Medicine* **35**, 201–219 (1979).

<sup>6</sup> N. Chan, M. Koritzinsky, H. Zhao, R. Bindra, P. M. Glazer, S. Powell, A. Belmaaza, B. Wouters, and R. G. Bristow, Chronic Hypoxia Decreases Synthesis of Homologous Recombination Proteins to Offset Chemoresistance and Radioresistance, *Cancer Research* **68**, 605–614 (2008).

<sup>7</sup> D. J. Chaplin, P. L. Olive, and R. E. Durand, Intermittent blood flow in a murine tumor: radiobiological effects., *Cancer Research* **47**, 597–601 (1987).

<sup>8</sup> M. W. Dewhirst, H. Kimura, S. W. Rehms, R. D. Braun, D. Papahadjopoulos, K. Hong, and T. W. Secomb, Microvascular studies on the origins of perfusion-limited hypoxia., *The British journal of cancer. Supplement* **27**, S247–51 (1996).

<sup>9</sup> H. Kimura, R. D. Braun, E. T. Ong, R. Hsu, T. W. Secomb, D. Papahadjopoulos, K. Hong, and M. W. Dewhirst, Fluctuations in red cell flux in tumor microvessels can lead to transient hypoxia and reoxygenation in tumor parenchyma., *Cancer Research* **56**, 5522–8 (1996).

<sup>10</sup> K. L. Bennewith and R. E. Durand, Quantifying Transient Hypoxia in Human Tumor Xenografts by Flow Cytometry, *Cancer Research* **64**, 6183–6189 (2004).

<sup>11</sup> S. B. Bader, M. W. Dewhirst, and E. M. Hammond, Cyclic Hypoxia: An Update on Its Characteristics, Methods to Measure It and Biological Implications in Cancer, *Cancers* **13**, 23 (2020).

<sup>12</sup> D. J. Carlson, R. D. Stewart, and V. A. Semenenko, Effects of oxygen on intrinsic radiation sensitivity: A test of the relationship between aerobic and hypoxic linear-quadratic (LQ) model parameters, *Medical Physics* **33**, 3105–3115 (2006).

<sup>13</sup> A. Daşu, I. Toma-Daşu, and M. Karlsson, The effects of hypoxia on the theoretical modelling of tumour control probability, *Acta Oncologica* **44**, 563–571 (2009).

<sup>14</sup> W. A. Tomé and J. F. Fowler, Selective boosting of tumor subvolumes, *International Journal of Radiation Oncology\*Biology\*Physics* **48**, 593–599 (2000).

<sup>15</sup> Å. Søvik, E. Malinen, Ø. S. Bruland, S. M. Bentzen, and D. R. Olsen, Optimization of tumour control probability in hypoxic tumours by radiation dose redistribution: a modelling study, *Physics in Medicine and Biology* **52**, 499–513 (2006).

<sup>16</sup> R. F. Kallman and M. J. Dorie, Tumor oxygenation and reoxygenation during radiation therapy: Their importance in predicting tumor response, *International Journal of Radiation Oncology\*Biology\*Physics* **12**, 681 – 685 (1986).

<sup>17</sup> E. Taylor, J. Zhou, P. Lindsay, W. Foltz, M. Cheung, I. Siddiqui, A. Hosni, A. E. Amir, J. Kim, R. P. Hill, D. A. Jaffray, and D. W. Hedley, Quantifying Reoxygenation in Pancreatic Cancer During Stereotactic Body Radiotherapy., *Scientific Reports* **10**, 1638 (2020).

<sup>18</sup> J. M. Brown, M. Diehn, and B. W. Loo, Stereotactic Ablative Radiotherapy Should Be Combined With a Hypoxic Cell Radiosensitizer, *International Journal of Radiation Oncology\*Biology\*Physics* **78**, 323–327 (2010).

<sup>19</sup> R. Ruggieri, S. Naccarato, and A. E. Nahum, Severe hypofractionation: Non-homogeneous tumour dose delivery can counteract tumour hypoxia, *Acta Oncologica* **49**, 1304–1314 (2010).

<sup>20</sup> D. J. Carlson, P. J. Keall, B. W. L. Jr, Z. J. Chen, and J. M. Brown, Hypofractionation Results in Reduced Tumor Cell Kill Compared to Conventional Fractionation for Tumors with Regions of Hypoxia, *International Journal of Radiation Oncology\*Biology\*Physics* **79**, 1188 – 1195 (2011).

<sup>21</sup> M. Kissick, D. Campos, A. v. d. Kogel, and R. Kimple, On the importance of prompt oxygen changes for hypofractionated radiation treatments, *Physics in Medicine and Biology* **58**, N279 (2013).

<sup>22</sup> E. Lindblom, L. Antonovic, A. Daşu, I. Lax, P. Wersäll, and I. Toma-Daşu, Treatment fractionation for stereotactic radiotherapy of lung tumours: a modelling study of the influence of chronic and acute hypoxia on tumour control probability, *Radiation Oncology* (London, England) **9**, 149–149 (2014).

<sup>23</sup> I. Toma-Daşu, H. Sandström, P. Barsoum, and A. Daşu, To fractionate or not to fractionate? That is the question for the radiosurgery of hypoxic tumors: Laboratory investigation, *Journal of Neurosurgery* **121**, 110–115 (2014).

<sup>24</sup> W. M. Harriss-Phillips, E. Bezak, and A. Potter, Stochastic Predictions of Cell Kill During Stereotactic Ablative Radiation Therapy: Do Hypoxia and Reoxygenation Really Matter?, *International Journal of Radiation Oncology\*Biology\*Physics* **95**, 1290–1297 (2016).

<sup>25</sup> J. Jeong, J. H. Oh, J.-J. Sonke, J. Belderbos, J. D. Bradley, A. N. Fontanella, S. S. Rao, and J. O. Deasy, Modeling the Cellular Response of Lung Cancer to Radiation Therapy for a Broad Range of Fractionation Schedules., *Clinical Cancer Research* **23**, 5469 – 5479 (2017).

<sup>26</sup> M. Guerrero and D. J. Carlson, A radiobiological model of reoxygenation and fractionation effects, *Medical Physics* **44**, 2002 – 2010 (2017).

<sup>27</sup> A. M. Elamir, T. Stanescu, A. Shessel, T. Tadic, I. Yeung, D. Letourneau, J. Kim, J. Lukovic, L. A. Dawson, R. Wong, A. Barry, J. Brierley, S. Gallinger, J. Knox, G. O’Kane, N. Dhani, A. Hosni, and E. Taylor, Simulated dose painting of hypoxic sub-volumes in pancreatic cancer stereotactic body radiotherapy, *Physics in Medicine & Biology* **66**, 185008 (2021).

<sup>28</sup> R. A. Popple, R. Ove, and S. Shen, Tumor control probability for selective boosting of hypoxic subvolumes, including the effect of reoxygenation, *International Journal of Radiation Oncology\*Biology\*Physics* **54**, 921–927 (2002).

<sup>29</sup> R. Ruggieri and A. E. Nahum, The impact of hypofractionation on simultaneous dose-boosting to hypoxic tumor subvolumes, *Medical Physics* **33**, 4044–4055 (2006).

<sup>30</sup> I. Toma-Daşu, A. Daşu, and A. Brahme, Dose prescription and optimisation based on tumour hypoxia, *Acta Oncologica* **48**, 1181–1192 (2009).

<sup>31</sup> J. Lanzen, R. D. Braun, B. Klitzman, D. Brizel, T. W. Secomb, and M. W. Dewhirst, Direct Demonstration of Instabilities in Oxygen Concentrations within the Extravascular Compartment of an Experimental Tumor, *Cancer Research* **66**, 2219–2223 (2006).

<sup>32</sup> R. H. Thomlinson and L. H. Gray, The histological structure of some human lung cancers and the possible implications for radiotherapy., *British Journal of Cancer* **9**, 539 – 549 (1955).

<sup>33</sup> S. F. Petit, A. L. A. J. Dekker, R. Seigneuric, L. Murrer, N. A. W. v. Riel, M. Nordmark, J. Overgaard, P. Lambin, and B. G. Wouters, Intra-voxel heterogeneity influences the dose prescription for dose-painting with radiotherapy: a modelling study, *Physics in Medicine and Biology* **54**, 2179–2196 (2009).

<sup>34</sup> A. Couvelard, D. O'Toole, H. Turley, R. Leek, A. Sauvanet, C. Degott, P. Ruszniewski, J. Belghiti, A. L. Harris, K. Gatter, and F. Pezzella, Microvascular density and hypoxia-inducible factor pathway in pancreatic endocrine tumours: negative correlation of microvascular density and VEGF expression with tumour progression, *British Journal of Cancer* **92**, 94–101 (2005).

<sup>35</sup> A. M. Schor, N. Pendleton, S. Pazouki, R. L. Smith, J. Morris, K. Lessan, E. Heerkens, L. M. Chandrachud, G. Carmichael, M. Adi, D. M. Chisholm, and H. Stevenson, Assessment of Vascularity in Histological Sections: Effects of Methodology and Value as an Index of Angiogenesis in Breast Tumours, *The Histochemical Journal* **30**, 849–856 (1998).

<sup>36</sup> T. Mäkitie, P. Summanen, A. Tarkkanen, and T. Kivelä, Microvascular density in predicting survival of patients with choroidal and ciliary body melanoma., *Investigative Ophthalmology & Visual science* **40**, 2471–80 (1999).

<sup>37</sup> N. Weidner, P. R. Carroll, J. Flax, W. Blumenfeld, and J. Folkman, Tumor angiogenesis correlates with metastasis in invasive prostate carcinoma., *The American Journal of Pathology* **143**, 401–9 (1993).

<sup>38</sup> A. M. Schor, S. Pazouki, J. Morris, R. L. Smither, L. M. Chandrachud, and N. Pendleton, Heterogeneity in microvascular density in lung tumours: comparison with normal bronchus., *British Journal of Cancer* **77**, 946–951 (1998).

<sup>39</sup> Z. Fuks and R. Kolesnick, Engaging the vascular component of the tumor response, *Cancer Cell* **8**, 89–91 (2005).

<sup>40</sup> V. Demidov, A. Maeda, M. Sugita, V. Madge, S. Sadanand, C. Flueraru, and I. A. Vitkin, Preclinical longitudinal imaging of tumor microvascular radiobiological response with functional optical coherence tomography, *Scientific Reports* **8**, 38 (2018).

<sup>41</sup> H. R. Withers, The Four R's of Radiotherapy, in *Advances in Radiation Biology*, edited by J. T. Lett and H. Adler, volume 5 of *Advances in Radiation Biology*, pages 241–271, Elsevier, 1975.

<sup>42</sup> I. Shuryak, D. J. Carlson, J. M. Brown, and D. J. Brenner, High-dose and fractionation effects in stereotactic radiation therapy: Analysis of tumor control data from 2965 patients, *Radiotherapy and Oncology* **115**, 327–334 (2015).

<sup>43</sup> Y. Shibamoto, A. Miyakawa, S. Otsuka, and H. Iwata, Radiobiology of hypofractionated stereotactic radiotherapy: what are the optimal fractionation schedules?, *Journal of Radiation Research* **57**, i76–i82 (2016).

<sup>44</sup> S. S. Ng, M. S. Ning, P. Lee, R. A. McMahon, S. Siva, and M. D. Chuong, Single-Fraction Stereotactic Body Radiation Therapy: A Paradigm During the Coronavirus Disease 2019 (COVID-19) Pandemic and Beyond?, *Advances in Radiation Oncology* **5**, 761–773 (2020).

<sup>45</sup> E. J. Hall and A. J. Giaccia, *Radiobiology for the Radiologist*, Wolters Kluwer Health, Philadelphia, 2011.

<sup>46</sup> A. Takeda, N. Sanuki, E. Kunieda, T. Ohashi, Y. Oku, T. Takeda, N. Shigematsu, and A. Kubo, Stereotactic Body Radiotherapy for Primary Lung Cancer at a Dose of

50 Gy Total in Five Fractions to the Periphery of the Planning Target Volume Calculated Using a Superposition Algorithm, *International Journal of Radiation Oncology\*Biology\*Physics* **73**, 442–448 (2009).

<sup>47</sup> G. M. Videtic, R. Paulus, A. K. Singh, J. Y. Chang, W. Parker, K. R. Olivier, R. D. Timmerman, R. R. Komaki, J. J. Urbanic, K. L. Stephans, S. S. Yom, C. G. Robinson, C. P. Belani, P. Iyengar, M. I. Ajlouni, D. D. Gopaul, J. B. G. Suescun, R. C. McGarry, H. Choy, and J. D. Bradley, Long-term Follow-up on NRG Oncology RTOG 0915 (NC-CTG N0927): A Randomized Phase 2 Study Comparing 2 Stereotactic Body Radiation Therapy Schedules for Medically Inoperable Patients With Stage I Peripheral Non-Small Cell Lung Cancer, *International Journal of Radiation Oncology\*Biology\*Physics* **103**, 1077–1084 (2019).

<sup>48</sup> A. K. Singh, J. A. Gomez-Suescun, K. L. Stephans, J. A. Bogart, G. M. Hermann, L. Tian, A. Groman, and G. M. Videtic, One Versus Three Fractions of Stereotactic Body Radiation Therapy for Peripheral Stage I to II Non-Small Cell Lung Cancer: A Randomized, Multi-Institution, Phase 2 Trial, *International Journal of Radiation Oncology\*Biology\*Physics* **105**, 752–759 (2019).

<sup>49</sup> P. T. Courtney, A. J. Paravati, T. F. Atwood, N. Raja, C. T. Zimmerman, P. T. Fanta, A. M. Lowy, D. R. Simpson, R. Xu, and J. D. Murphy, Phase I Trial of Stereotactic Body Radiation Therapy Dose Escalation in Pancreatic Cancer, *International Journal of Radiation Oncology\*Biology\*Physics* **110**, 1003–1012 (2021).

<sup>50</sup> L. Henke, R. Kashani, C. Robinson, A. Curcuru, T. DeWees, J. Bradley, O. Green, J. Michalski, S. Mutic, P. Parikh, and J. Olsen, Phase I trial of stereotactic MR-guided online adaptive radiation therapy (SMART) for the treatment of oligometastatic or unresectable primary malignancies of the abdomen, *Radiotherapy and Oncology* **126**, 519 – 526 (2018).

<sup>51</sup> A. Mahadevan, R. Miksad, M. Goldstein, R. Sullivan, A. Bullock, E. Buchbinder, D. Pleskow, M. Sawhney, T. Kent, C. Vollmer, and M. Callery, Induction Gemcitabine and Stereotactic Body Radiotherapy for Locally Advanced Nonmetastatic Pancreas Cancer, *International Journal of Radiation Oncology\*Biology\*Physics* **81**, e615–e622 (2011).

<sup>52</sup> A. C. Koong, Q. T. Le, A. Ho, B. Fong, G. Fisher, C. Cho, J. Ford, J. Poen, I. C. Gibbs, V. K. Mehta, S. Kee, W. Trueblood, G. Yang, and J. A. Bastidas, Phase I study of stereotactic radiosurgery in patients with locally advanced pancreatic cancer, *International Journal of Radiation Oncology\*Biology\*Physics* **58**, 1017 – 1021 (2004).

<sup>53</sup> A. Takeda, N. Sanuki, T. Eriguchi, T. Kobayashi, S. Iwabuchi, K. Matsunaga, T. Mizuno, K. Yashiro, S. Nisimura, and E. Kunieda, Stereotactic ablative body radiotherapy for previously untreated solitary hepatocellular carcinoma, *Journal of Gastroenterology and Hepatology* **29**, 372–379 (2014).

<sup>54</sup> N. Sanuki, A. Takeda, T. Mizuno, Y. Oku, T. Eriguchi, S. Iwabuchi, and E. Kunieda, Tumor Response on CT Following Hypofractionated Stereotactic Ablative Body Radiotherapy for Small Hypervascular Hepatocellular Carcinoma With Cirrhosis, *American Journal of Roentgenology* **201**, W812–W820 (2013).

<sup>55</sup> J.-E. Bibault, S. Dewas, C. Vautravers-Dewas, A. Hollebecque, H. Jarraya, T. Lacornerie, E. Lartigau, and X. Mirabel, Stereotactic Body Radiation Therapy for Hepatocellular Carcinoma: Prognostic Factors of Local Control, Overall Survival, and Toxicity, *PLoS ONE* **8**, e77472 (2013).

<sup>56</sup> D. L. Andolino, C. S. Johnson, M. Maluccio, P. Kwo, A. J. Tector, J. Zook, P. A. Johnstone, and H. R. Cardenes, Stereotactic Body Radiotherapy for Primary Hepatocellular Carcinoma, *International Journal of Radiation Oncology\*Biology\*Physics* **81**, e447–e453 (2011).

<sup>57</sup> A. Widmark, A. Gunnlaugsson, L. Beckman, C. Thellenberg-Karlsson, M. Hoyer, M. Lagerlund, J. Kindblom, C. Ginman, B. Johansson, K. Björnlinger, M. Seke, M. Agrup, P. Fransson, B. Tavelin, D. Norman, B. Zackrisson, H. Anderson, E. Kjellén, L. Franzén, and P. Nilsson, Ultra-hypofractionated versus conventionally fractionated radiotherapy for prostate cancer: 5-year outcomes of the HYPO-RT-PC randomised, non-inferiority, phase 3 trial, *The Lancet* **394**, 385–395 (2019).

<sup>58</sup> D. H. Brand et al., Intensity-modulated fractionated radiotherapy versus stereotactic body radiotherapy for prostate cancer (PACE-B): acute toxicity findings from an international, randomised, open-label, phase 3, non-inferiority trial, *The Lancet. Oncology* **20**, 1531–1543 (2019).

<sup>59</sup> T. Zilli, C. Franzese, M. Bottero, N. Giaj-Levra, R. Förster, D. Zwahlen, N. Koutsouvelis, A. Bertaut, J. Blanc, G. R. D'agostino, F. Alongi, M. Guckenberger, M. Scorsetti, and R. Miralbell, Single fraction urethra-sparing prostate cancer SBRT: Phase I results of the ONE SHOT trial, *Radiotherapy and Oncology* **139**, 83–86 (2019).

<sup>60</sup> R. Nath, W. S. Bice, W. M. Butler, Z. Chen, A. S. Meigooni, V. Narayana, M. J. Rivard, Y. Yu, and A. A. o. P. i. Medicine, AAPM recommendations on dose prescription and reporting methods for permanent interstitial brachytherapy for prostate cancer: Report of Task Group 137, *Medical Physics* **36**, 5310–5322 (2009).

<sup>61</sup> N. Ohri, W. A. Tomé, A. M. Romero, M. Miften, R. K. T. Haken, L. A. Dawson, J. Grimm, E. Yorke, and A. Jackson, Local Control After Stereotactic Body Radiation Therapy for Liver Tumors, *International Journal of Radiation Oncology\*Biology\*Physics* **110**, 188–195 (2021).

<sup>62</sup> S. K. Schaub, P. E. Hartvigson, M. I. Lock, M. Høyter, T. B. Brunner, H. R. Cardenes, L. A. Dawson, E. Y. Kim, N. A. Mayr, S. S. Lo, and S. Apisarnthanarax, Stereotactic Body Radiation Therapy for Hepatocellular Carcinoma: Current Trends and Controversies, *Technology in Cancer Research & Treatment* **17**, 1533033818790217 (2018).

<sup>63</sup> G. Morton, M. McGuffin, H. T. Chung, C.-L. Tseng, J. Helou, A. Ravi, P. Cheung, E. Szumacher, S. Liu, W. Chu, L. Zhang, A. Mamedov, and A. Loblaw, Prostate high dose-rate brachytherapy as monotherapy for low and intermediate risk prostate cancer: Efficacy results from a randomized phase II clinical trial of one fraction of 19 Gy or two fractions of 13.5 Gy, *Radiotherapy and Oncology* **146**, 90–96 (2020).

<sup>64</sup> J. P. Kirkpatrick, J. J. Meyer, and L. B. Marks, The Linear-Quadratic Model Is Inappropriate to Model High Dose per Fraction Effects in Radiosurgery, *Seminars in Radiation Oncology* **18**, 240–243 (2008), Hypofractionation.

<sup>65</sup> D. J. Brenner, The Linear-Quadratic Model Is an Appropriate Methodology for Determining Isoeffective Doses at Large Doses Per Fraction, *Seminars in Radiation Oncology* **18**, 234–239 (2008), Hypofractionation.

<sup>66</sup> E. Lindblom, A. Daşu, I. Lax, and I. Toma-Daşu, Survival and tumour control probability in tumours with heterogeneous oxygenation: A comparison between the linear-

quadratic and the universal survival curve models for high doses, *Acta Oncologica* **53**, 1035–1040 (2014).

<sup>67</sup> N. Crokart, B. F. Jordan, C. Baudelet, R. Ansiaux, P. Sonveaux, V. Grégoire, N. Beghein, J. DeWever, C. Bouzin, O. Feron, and B. Gallez, Early reoxygenation in tumors after irradiation: Determining factors and consequences for radiotherapy regimens using daily multiple fractions, *International Journal of Radiation Oncology\*Biology\*Physics* **63**, 901 – 910 (2005).

<sup>68</sup> J. Bussink, J. H. Kaanders, P. F. Rijken, J. A. Raleigh, and A. J. v. d. Kogel, Changes in blood perfusion and hypoxia after irradiation of a human squamous cell carcinoma xenograft tumor line., *Radiation Research* **153**, 398 – 404 (2000).

<sup>69</sup> O. J. Kelada, R. H. Decker, S. K. Nath, K. L. Johung, M.-Q. Zheng, Y. Huang, J.-D. Gallezot, C. Liu, R. E. Carson, U. Oelfke, and D. J. Carlson, High Single Doses of Radiation May Induce Elevated Levels of Hypoxia in Early-Stage Non-Small Cell Lung Cancer Tumors, *International Journal of Radiation Oncology\*Biology\*Physics* **102**, 174 – 183 (2018).

<sup>70</sup> K. Chao, W. R. Bosch, S. Mutic, J. S. Lewis, F. Dehdashti, M. A. Mintun, J. F. Dempsey, C. A. Perez, J. A. Purdy, and M. J. Welch, A novel approach to overcome hypoxic tumor resistance: Cu-ATSM-guided intensity-modulated radiation therapy, *International Journal of Radiation Oncology\*Biology\*Physics* **49**, 1171–1182 (2001).

<sup>71</sup> E. Malinen, Å. Søvik, D. Hristov, Ø. S. Bruland, and D. R. Olsen, Adapting radiotherapy to hypoxic tumours, *Physics in Medicine and Biology* **51**, 4903–4921 (2006).

<sup>72</sup> D. Thorwarth, S.-M. Eschmann, F. Paulsen, and M. Alber, Hypoxia Dose Painting by Numbers: A Planning Study, *International Journal of Radiation Oncology\*Biology\*Physics* **68**, 291–300 (2007).

<sup>73</sup> D. Mönnich, E. G. Troost, J. H. Kaanders, W. J. Oyen, M. Alber, and D. Thorwarth, Modelling and simulation of the influence of acute and chronic hypoxia on [<sup>18</sup>F]fluoromisonidazole PET imaging, *Physics in Medicine and Biology* **57**, 1675 – 1684 (2012).

<sup>74</sup> B. Wang, Z. Q. Gao, and X. Yan, Correlative study of angiogenesis and dynamic contrast-enhanced magnetic resonance imaging features of hepatocellular carcinoma, *Acta Radiologica* **46**, 353–358 (2005), PMID: 16134309.

<sup>75</sup> Y. Hattori, T. Gabata, O. Matsui, K. Mochizuki, H. Kitagawa, M. Kayahara, T. Ohta, and Y. Nakanuma, Enhancement patterns of pancreatic adenocarcinoma on conventional dynamic multi-detector row CT: Correlation with angiogenesis and fibrosis, *World Journal of Gastroenterology* **15**, 3114–3121 (2009).

<sup>76</sup> D. Thorwarth, S.-M. Eschmann, J. Scheiderbauer, F. Paulsen, and M. Alber, Kinetic analysis of dynamic <sup>18</sup>F-fluoromisonidazole PET correlates with radiation treatment outcome in head-and-neck cancer., *BMC Cancer* **5**, 152 (2005).

<sup>77</sup> D. Yan, S. Chen, D. J. Krauss, P. Y. Chen, P. Chinnaiyan, and G. D. Wilson, Tumor Voxel Dose-Response Matrix and Dose Prescription Function Derived Using <sup>18</sup>F-FDG PET/CT Images for Adaptive Dose Painting by Number, *International Journal of Radiation Oncology\*Biology\*Physics* **104**, 207–218 (2019).